Numerical simulations of the decay of primordial magnetic turbulence

Tina Kahniashvili,[1,2,3,*] Axel Brandenburg,[4,5,†] Alexander G. Tevzadze,[3,6,‡] and Bharat Ratra[7,§]

[1]*McWilliams Center for Cosmology and Department of Physics, Carnegie Mellon University, 5000 Forbes Ave, Pittsburgh, Pennsylvania 15213, USA*
[2]*Department of Physics, Laurentian University, Ramsey Lake Road, Sudbury, ON P3E 2C, Canada*
[3]*Abastumani Astrophysical Observatory, Ilia State University, 2A Kazbegi Ave, Tbilisi, GE-0160, Georgia*
[4]*Nordita, AlbaNova University Center, Roslagstullsbacken 23, 10691 Stockholm, Sweden*
[5]*Department of Astronomy, Stockholm University, SE 10691 Stockholm, Sweden*
[6]*Faculty of Exact and Natural Sciences, Tbilisi State University, 1 Chavchavadze Avenue Tbilisi, GE-0128, Georgia*
[7]*Department of Physics, Kansas State University, 116 Cardwell Hall, Manhattan, Kansas 66506, USA*
(Received 19 April 2010; published 1 June 2010)

We perform direct numerical simulations of forced and freely decaying 3D magnetohydrodynamic turbulence in order to model magnetic field evolution during cosmological phase transitions in the early Universe. Our approach assumes the existence of a magnetic field generated either by a process during inflation or shortly thereafter, or by bubble collisions during a phase transition. We show that the final configuration of the magnetic field depends on the initial conditions, while the velocity field is nearly independent of initial conditions.

I. INTRODUCTION

Astronomical observations show that galaxies have magnetic fields with a component that is coherent over a large fraction of the galaxy with field strengths of order 10^{-6} Gauss (G); see Refs. [1–4] and references therein.[1] Modeling the origin of these fields is a challenging problem. Here we consider models in which the seed field is generated in the early Universe, see, e.g. [1,3,6]. There are a number of such models and different models result in different magnetic field structures.

It is well known that quantum-mechanical fluctuations during inflation can generate energy-density inhomogeneities that seed observed large-scale structure, see, e.g., Ref. [7]. Quantum-mechanical zero-point fluctuations can also generate a seed magnetic field, provided the relevant Abelian gauge field is such that the Lagrangian density is not conformally invariant during inflation [8–10]. A seed magnetic field generated during inflation has a correlation length today that can be very much larger than the current Hubble radius. A convenient phenomenological way of breaking conformal invariance during inflation is to couple the inflaton scalar field ϕ to the vector Abelian gauge field

by $e^{\alpha\phi}F_{\mu\nu}F^{\mu\nu}$, where $F_{\mu\nu}$ is the vector field strength tensor and α is a parameter [9]. Depending on the value of α, this can result in a sufficiently large seed magnetic field to explain the observed galactic magnetic fields. This is a classically consistent model, with vector field back-reaction during inflation being negligibly small [9,11]. While the Abelian gauge field becomes strongly coupled at early times [9,11,12], this is not a problem for the effective, phenomenological, classical model, [9,11,12] and also see [6,13]. Of course, just as one does not reject the effective, phenomenological, classical "standard" ΛCDM cosmological model, one does not reject inflation-based seed magnetic field generation models for being quantum-mechanically inconsistent. Rather, much as the case for ΛCDM, it is of great interest to understand how such a successful inflation-based seed magnetic field generation model might arise from a more fundamental underlying model or theory.

There are a number of other seed field generation models; see Ref. [14] for a discussion of seed field generation in Hořava-Lifshitz gravity. Yet another interesting possibility is primordial magnetic field generation during a cosmological phase transition [15]. If the phase transition takes place at late times the magnetic field correlation length is smaller than the Hubble radius.

If the magnetic field was generated during or shortly after inflation (during a pre- or reheating phase transition), and survived to the epoch of recombination (the last-scattering surface), it should leave observable signatures on the cosmic microwave background (CMB) radiation

*tinatin@phys.ksu.edu
†brandenb@nordita.org
‡aleko@tevza.org
§ratra@phys.ksu.edu
[1]See Ref. [5] and references therein for a technique that might soon prove useful for measuring a larger-scale, cosmological, magnetic field.

fluctuations, see Ref. [16] for a review and Refs. [17,18] for more recent discussions.[2]

The shape and magnitude of a primordial magnetic field can be constrained observationally. Magnetic field energy-density scales like radiation (i.e. relativistic) energy density.[3] During nucleosynthesis, any new form of radiation-like energy density is constrained observationally to be less than about 10% of the usual radiation energy density. Hence, agreement between the big bang nucleosynthesis (BBN) model light nuclei abundance predictions and the observations yields a constraint on the primordial magnetic field energy density: $\Omega_B h_0^2 \lesssim 2.4 \times 10^{-6}$ [21]. Here Ω_B is the current value of the magnetic field energy density parameter and h_0 is the current value of the Hubble parameter in units of $100 \text{ km s}^{-1} \text{ Mpc}^{-1}$. Naturally, this limit holds only if the primordial magnetic field was generated prior to or during nucleosynthesis.

Other constraints arise through the effects of a primordial magnetic field on the propagation of CMB photons (Faraday rotation of the CMB polarization [18], and magnetic field induced scalar, vector, and tensor modes of CMB anisotropies [16,17]). Available data limit the current value of a cosmological magnetic field to be less than about 10^{-8} G for a scale-invariant or homogeneous primordial magnetic field.

Another interesting signature of a primordial magnetic field is relic gravitational waves generated by the anisotropic magnetic stress [22]. The amplitude of the gravitational wave signal is determined by the efficiency of gravitational wave generation and the strength of the primordial magnetic field. The efficiency of gravitational wave production is small [23] due to the small value of the Newton constant G in the coupling between the primordial magnetic field and the gravitational waves. However, a magnetic field that satisfies the BBN limit and that is generated during a strong-enough first-order phase transition can lead to a detectable signal for LISA. Therefore, the direct measurement of the gravitational wave background can lead to an independent limit on a magnetic field generated in the early Universe [24].

On large scales, because of the high conductivity of the plasma in the early Universe, the magnetic field is treated as a frozen-in field with its evolution determined by the simple dilution of magnetic field lines, $\mathbf{B}(\mathbf{x}, t) \propto \mathbf{B}(\mathbf{x})/a^2(t)$, where t is the physical cosmic time and $a(t)$ is

the scale factor. In general, however, the evolution of a primordial magnetic field is a complex process influenced by MHD as well as by cosmological dynamics [25]. In particular, the presence of a magnetic field can dramatically affect the behavior of primordial turbulence (for example, turbulence associated with phase transition bubble motions) [26–28]. Also, the presence of a magnetic field might itself lead to the development of turbulent motions, see Refs. [29–31] and Sec. III below.

In this paper we study the evolution of a primordial magnetic field that is coupled, through the MHD equations, with the fluid, during a cosmological phase transition. We consider two different possibilities: (i) when the magnetic field energy has been injected in the plasma with no initial vorticity perturbations (no turbulent motions) at a given typical scale; and, (ii) when vorticity perturbations are present during the phase transition and couple to the magnetic field with a given spectrum. Both these assumptions can be justified. The magnetic field might be generated prior to the phase transition, with the generation mechanism not requiring turbulent motion. On the other hand, the presence of initial turbulent motions can also be justified since bubble nucleation, expansion, and collisions can lead to primordial kinetic turbulence [32]. Of course, in reality both magnetic field and kinetic turbulence generation can take place together, while in our approach we assume the *a priori* presence of magnetic energy and/or kinetic energy during the phase transition.

A causal, phenomenological description of MHD on large scales during the cosmological phase transition motivates a white noise spectrum for the magnetic spectral energy density, $E_M(k) \propto k^2$, where k is the wave number [33]. A steeper Batchelor spectrum with $E_M(k) \propto k^4$ has been claimed to follow from cosmological causality and the divergenceless condition of the magnetic field [34]. To understand the evolution of a cosmological magnetic field, and to be able to make observable predictions in this model, it is important to resolve this impasse. One would like to know whether the final large-scale magnetic energy spectrum evolves to something steeper than white noise, or to a spectrum closer to the Batchelor one.

In fact, the MHD process itself might establish a different spectrum: The possibility of generating a random magnetic field from isotropic turbulence was first proposed by Batchelor [35]. He invoked the imperfect analogy between vorticity and magnetic fields that should generally imply a large-scale distribution of the magnetic energy similar to the kinetic energy of turbulent motions $E_K(k) \propto k^4$ [36]. Later, Kazantsev [37] was able to rigorously establish the possibility of small-scale dynamo action. He assumed that the velocity field varied only on large scales and found that weak magnetic fields are amplified mainly on the resistive scale. Initially, this was thought to be applicable only to turbulence at large magnetic Prandtl number [38], where the viscous cutoff scale is much larger than the resistive

---

[2] A potential advantage of a primordial seed field that is coherent over scales larger than the current Hubble radius, as can be generated by inflation, is that it might be able to explain some of the large-scale oddities of the observed CMB temperature anisotropy [19], including potential non-Gaussianity [20].

[3] The ratio of the magnetic field energy density ρ_B and the energy density of radiation ρ_{rad} is constant during cosmological evolution, if the primordial magnetic is not damped by MHD (or other) processes and so stays frozen into the plasma.

cutoff scale. Kazantsev found that the magnetic energy spectrum increases with wave number like $k^{3/2}$, which is slightly shallower than the white noise spectrum k^2. The emergence of a Kazantsev spectrum turned out to be much more ubiquitous and not only applicable at large magnetic Prandtl number. Simulations at magnetic Prandtl numbers of order unity also clearly showed the Kazantsev $k^{3/2}$ spectrum [27]. Such a spectrum could be of interest for primordial magnetic field evolution, because it implies somewhat larger power at large scales than white noise.

The main goal of our paper is to determine, through MHD modeling, the evolution of the magnetic energy spectrum. To keep our study as general as possible we do not make any assumption about the physical process leading to primordial magnetic field generation. Also, we do not address the phase transition physics itself, keeping the total magnetic field energy density ρ_B as a free parameter whose maximal value is fixed by the BBN bound. Obviously, if the magnetic field is generated during a phase transition, ρ_B will depend sensitively on the amount of latent heat that is transformed to magnetic energy, i.e. on the efficiency of the magnetic field generation process. One important issue addressed here is to determine the spectral shape of the magnetic field at large scales, assuming that magnetic energy and vorticity perturbations are closely coupled during the phase transition. Another important question is related to the duration of MHD turbulence and how long it takes to reach equipartition between kinetic and magnetic energy densities in the primordial plasma.

The structure of this paper is as follows. In Sec. II we describe the model, defining the main model parameters (Sec. II A), characterizing the magnetic field spectrum (Sec. II B), and formulating initial conditions (Sec. II C). In Sec. III we present results from direct 3D MHD simulations performed using the PENCIL CODE [39]. We conclude in Sec. IV. We employ natural units with $\hbar = 1 = c$ and Gaussian units for electromagnetic quantities. To properly account for the expansion of the Universe we use comoving quantities with conformal time t that is related to physical time t_{phys} as $t \propto t_{\mathrm{phys}}^{1/2}$ during the radiation dominated epoch.

II. MODEL DESCRIPTION

We assume that magnetic energy is generated at the electroweak or QCD phase transition, or during inflation. In the first case magnetic energy is explicitly injected into the fluid on small length scales, smaller than the Hubble length at the moment of the phase transition. If the magnetic field originated at an earlier epoch of inflation the length scale at which the magnetic field interacts with the fluid is set by the characteristic length scale of the system, and is again smaller than the Hubble radius. In the absence of magnetic or kinetic helicity we do not expect an inverse

cascade (i.e., energy flow from smaller to larger length scales).

A. Phase transition characteristics

To model magnetic field evolution one needs to know the physical conditions during the phase transition. First, generation of turbulence requires a first-order phase transition so that at the critical temperature of the phase transition bubbles of the new vacuum nucleate within the false vacuum. Bubble collisions then generate turbulent motions. The standard electroweak model does not have a first-order phase transition [40], and cannot account for baryogenesis. However, modifications of the standard model, such as the minimal supersymmetric standard model (MSSM) [41], result in first-order electroweak phase transitions and can account for baryogenesis [42]. Also, recent lattice QCD computations [43] have not yet excluded that the QCD phase transition is a first-order one, with bubble nucleation and collisions.

The main parameter characterizing turbulent motions is the root mean square (r.m.s.) velocity v_0 which determines the kinetic energy density of the turbulence. Obviously, v_0 depends sensitively on the phase transition physics, and, in particular, on the phase transition bubble wall expansion velocity v_b, [44]. To model the development of turbulent motions during the phase transition we adapt earlier analytical or semianalytical results [44,45]. The first question that must be answered is whether the phase transition is first order, and, if so, what fraction of total available vacuum energy is transformed into kinetic energy of the bubbles. The r.m.s. velocity of the turbulent motions can be approximated as (see Ref. [45])

$$v_0 = \sqrt{\frac{3\kappa\alpha}{4 + 3\kappa\alpha}}. \qquad (1)$$

Here $\alpha = \rho_{\mathrm{vac}}/\rho_{\mathrm{thermal}}$ is the ratio of the vacuum energy density associated with the phase transition to the thermal energy density of the Universe at the time (α characterizes the strength of the phase transition), and the efficiency factor κ is the fraction of the available vacuum energy that goes into the kinetic energy of the expanding bubble walls (as opposed to thermal energy).

On the other hand, the primordial magnetic field is characterized by the r.m.s. Alfvén velocity given by

$$v_A = \frac{B}{\sqrt{4\pi w_{\mathrm{rad}}}} = \sqrt{\frac{3\rho_B}{2\rho_{\mathrm{rad}}}} \simeq 7.65 \times 10^2 \sqrt{\Omega_B}. \qquad (2)$$

Here $w_{\mathrm{rad}} = 4\rho_{\mathrm{rad}}/3$ (with $\rho_{\mathrm{rad}} \simeq \rho_{\mathrm{thermal}}$) is the radiation enthalpy of the relativistic fluid and we have used $\Omega_{\mathrm{rad}} h_0^2 = 2.56 \times 10^{-5}$ for a present-day CMB temperature $T_0 = 2.74$ K. At temperature $T_\star$ of the phase transition we have $\rho_{\mathrm{rad}}(T_\star) = \pi^2 g_*(T_*)^4/30$, where $g_\star$ is the number of

relativistic degrees of freedom at temperature $T_\star$. The r.m.s. Alfvén velocity does not depend on $T_\star$, but it is weakly dependent on $g_\star$,

$$v_A \simeq 4 \times 10^{-4} \left(\frac{B}{10^{-9}\,\mathrm{G}}\right)\left(\frac{g_\star}{100}\right)^{-1/6}. \tag{3}$$

Assuming equipartition between kinetic and magnetic energy densities, one has $v_A \simeq v_0$. While the equipartition condition can be justified by MHD dimensional analysis [29], we explicitly show that it holds by performing a 3D direct numerical simulation of a primordial magnetic field coupled to fluid motions; see Sec. III. Also, partial equipartition, $v_0 \sim 0.8 v_A$, is reached in the case where the magnetic field was generated first at the injection scale, which then led to rapid growth of vorticity perturbations in the initially no-turbulent plasma.

The bubble wall expansion sets the maximal size of the bubble, which we associate with the size of the largest turbulent eddy, $l_0 = v_b \beta^{-1}$, where β is a parameter that characterizes the duration of the phase transition. In particular, β can be obtained from the bubble nucleation rate [32]. The Hubble time $H_\star^{-1}$ at the phase transition is another characteristic time, and it sets the "causality" horizon. At this point it is useful to define the parameter $\gamma[= l_0 H_\star = v_b (\beta/H_\star)^{-1}]$ which determines how many maximal-sized bubbles are within the Hubble radius, $N \approx \gamma^3$.

B. Magnetic field spectrum

If a primordial magnetic field is randomly oriented and its mean value vanishes, i.e. $\langle \mathbf{B}(\mathbf{x}) \rangle = 0$, it is conveniently described statistically in terms of the n-point field correlation functions. If the field is isotropic with a Gaussian distribution, the magnetic field characteristics are completely determined by the two-point correlation function $\langle \mathbf{B}(\mathbf{x} + \mathbf{r}, t + \tau)\mathbf{B}(\mathbf{x}, t) \rangle$. To construct this main characteristic function we need to know the spatial distribution (i.e., the correlation length) and the temporal evolution of the magnetic field.

When considering a causally generated primordial magnetic field, its maximal comoving correlation length $\xi_{\max}$ is set by the comoving Hubble radius $\lambda_H (= H_\star^{-1} a_0/a_\star)$ at the moment of generation (here a_0 and $a_\star$ are the scale factors today and at magnetic field generation, respectively). Causality implies that

$$\xi_{\max} \leq \lambda_H = 5.8 \times 10^{-10}\,\mathrm{Mpc}\left(\frac{100\,\mathrm{GeV}}{T_\star}\right)\left(\frac{100}{g_\star}\right)^{1/6}, \tag{4}$$

where the temperature $T_\star$ corresponds to the energy scale at field generation. For the electroweak phase transition, $T_\star$ is related to the Higgs mass M_H through $T_\star \simeq (1.2 \pm 0.2)M_H$, so we parameterize the $T_\star$ dependence by normal-

izing to a temperature of 100 GeV. Also, for the electroweak phase transition $g_\star \simeq 100$, but the dependence on $g_\star$ is much weaker than the $T_\star$ dependence.

Another way to determine the magnetic field correlation length is to use the magnetic energy spectrum[4] $E_M(k, t)$, defining the correlation length by $\xi_M(t) = [\int_0^\infty dk\, k^{-1} E_M(k, t)]/\int_0^\infty dk\, E_M(k, t)$.

In most models of magnetic field generation during a phase transition [15], the magnetic field correlation length is determined by the phase transition's bubble sizes. In this case a characteristic magnetic field correlation length is assumed to be determined by the largest bubble, $\lambda_0 \simeq \gamma \lambda_H$. This simple dimensional description implies that the magnetic energy density ρ_B is redistributed through MHD processes and establishes a magnetic spectrum with spectral energy density measured today that is given by [23]

$$E_M(k) \leq \frac{5.2(\alpha + 1)}{3\alpha + 5}\left(\frac{100\,\mathrm{GeV}}{T_\star}\right)\left(\frac{100}{g_\star}\right)^{1/2} \gamma \frac{(10^{-9}\,\mathrm{G})^2}{\mathrm{pc}^{-1}}$$
$$\times \left\{ \begin{array}{ll} \bar{k}^\alpha & \text{if } \bar{k} < 1 \\ \bar{k}^{-5/3} & \text{if } \bar{k} > 1 \end{array} \right\}. \tag{7}$$

Here, $\bar{k} = k/k_0$ and $\bar{k}_D = k_D/k_0$ with $k_0 = 2\pi/\lambda_0$, and $k_D = 2\pi/\lambda_D$ is the damping wave number determined through the viscosity-driven dissipation of the magnetic field. In the case of stationary nonhelical Kolmogorov turbulence the Reynolds number determines the damping scale k_D as $\mathrm{Re} = (k_D/k_0)^{4/3}$. Note that the Reynolds number is high enough in the early Universe to ensure the presence of a wide inertial (turbulent) range, $k_0 < k < k_D$.[5] The large-scale behavior of the magnetic field is determined by the parameter α. The scale-invariant spectrum corresponds to $\alpha = -1$ [9], the Kazantsev spectrum has $\alpha = 3/2$ [37], the white noise spectrum corresponds to $\alpha = 2$ [33], and the steep Batchelor spectrum has $\alpha = 4$ [35]. Equation (7) does not account for any damping of magnetic energy and can be viewed as the

---

[4]In what follows we use [46]

$$\langle B_i^*(\mathbf{k}, t)B_j(\mathbf{k}', t + \tau) \rangle = \delta(\mathbf{k} - \mathbf{k}')F_{ij}^M(\mathbf{k}, t)f[\eta(k), \tau], \tag{5}$$

where

$$8\pi k^2 F_{ij}^M(\mathbf{k}, \tau) = 2P_{ij}(\mathbf{k})E_M(k, t) + i\varepsilon_{ijl}k_l H_M(k, t). \tag{6}$$

Here $P_{ij}(\mathbf{k}) = \delta_{ij} - k_i k_j/k^2$ is the projection operator, δ_{ij} is the Kronecker delta, $k = |\mathbf{k}|$, ε_{ijl} is the totally antisymmetric tensor, and $\eta(k)$ is an autocorrelation function that determines the characteristic function $f[\eta(k), \tau]$ describing the temporal decorrelation of turbulent fluctuations. The scalar function $H_M(k, t)$ is the magnetic helicity spectrum. All configurations of the helical magnetic field must satisfy the "realizability condition" [29,30], $|\int_0^\infty dk H_M(k, t)| \leq 2\xi_M(t)\mathcal{E}_M(t)$.

[5]References [28] have recently analytically estimated the Reynolds number in the early Universe at the scale of energy injection of the turbulence and magnetic field.
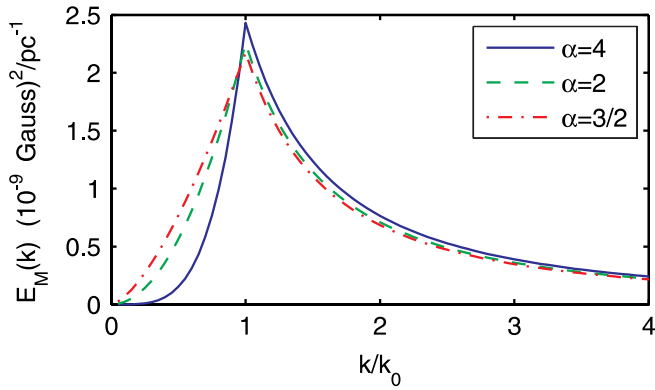
FIG. 1 (color online).   The maximal allowed value $E_M(k)$ of the magnetic field generated during the EW phase transition with $T_\star = 100$ Gev, $g_\star = 100$, and $\gamma = 0.01$.

BBN bound imposed at the moment of the establishment of the magnetic spectrum; see Fig. 1.

C. MHD formalism and initial conditions

As discussed in Ref. [47], the usual relativistic MHD equations are identical to the MHD equations in an expanding Universe with zero spatial curvature when physical quantities are replaced by their comoving counterparts and conformal time η is used in place of physical time. Based on this fact, we perform direct numerical simulations of MHD turbulence in the expanding Universe using the usual MHD equations for an ultrarelativistic equation of state, but nonrelativistic bulk motions.

The characteristic length-scale of the problem is set by the phase transition bubble size $\gamma \lambda_H$. The typical time-scale is the eddy turnover time. Assuming that turbulent eddies correspond to phase transition bubbles, the *physical* turnover time is $\tau_0 \sim (v_b/v_0)(\beta/H_\star)^{-1}$, where $v_0 = \langle V^2 \rangle^{1/2}$.

Another characteristic of the initial stage is the amount of magnetic and kinetic energies present during the phase transition, i.e. the initial Alfvén and turbulent r.m.s. velocities. As discussed above, both quantities are sensitively dependent on the available vacuum energy that is converted to magnetic energy (if the magnetic field was generated during the phase transition) and/or the kinetic energy of the turbulent motions. In our analysis below we assume that about 10% of the vacuum energy is in the form of initial magnetic energy, which corresponds to $v_{A,\text{in}} \simeq 0.3$.

We perform the numerical simulations of magnetic field evolution in two stages. During the first stage, we model *forced* MHD turbulence with injection of energy at fixed wave number. This type of driving force is supposed to mimic the action of bubble-induced external forces in MHD turbulence during the phase transition. The simulation of forced MHD turbulence is carried out before equipartition is reached, i.e., before $v_0 \sim v_A$. After equi-

partition is reached we switch off the driving force and allow *free decay* of the turbulent state.

We use two different types of external forcing during the first stage of the simulations. These are injecting magnetic or kinetic energy at a given scale associated with the turbulent eddy size. These cases differ in the initial magnetic field configuration. Injection of the magnetic energy in the flow is achieved by using a delta function spectral energy-density function for the magnetic field. Injection of the kinetic energy is achieved by using a delta function spectral energy-density function for the velocity field. In the latter case the spectral energy distribution of the initial magnetic field is of Batchelor's type ($E_B \propto k^4$) and its amplitude is close to that of the kinetic energy density (the equipartition condition).

We also define the spectrum of the velocity field $E_K(k, t)$ and the total energy density $\mathcal{E}_K(t) = \int_0^\infty E_K(k, t)dk$. One of our main goals is to determine whether the presence of magnetic fields in the early Universe (e.g. generated prior to a phase transition) can lead to strong turbulence.

III. NUMERICAL SIMULATIONS

Numerical simulations of the magnetic field evolution were performed using the PENCIL CODE [27,48–50]; see [39] for the web site.

We perform all simulations using comoving quantities and conformal time. For simplicity we work with dimensionless quantities, and use $k_1 = k_0/30$ as our wave number unit. The chosen box size covers a wave number range from $k_0/30$ up to $4.3 \times k_0$, and the maximal length scale considered corresponds to $\lambda_1 = 30\gamma\lambda_H$, which is still within the electroweak phase transition Hubble scale ($\gamma_{\text{EW}} \lesssim 0.01$). In the case of a QCD phase transition for an extremely large QCD bubble velocity, $v_b \rightarrow 1$, the scale can exceed the QCD phase transition Hubble scale by a factor of 2 ($\gamma_{\text{QCD}} \lesssim 0.15$). Of course, in the simulations we have to use a relatively large value for the dissipation wave number, which is $k_D \simeq 2k_0$ at the end of the simulation. This high value is a consequence of choosing a constant viscosity that must be large enough so that it can also cope with the initially much larger value of the energy dissipation rate. Such high values are obviously not realistic for the early Universe where the Reynolds number is extremely high. However, we motivate this choice by the fact that we are mainly interested in the evolution of the magnetic field outside the inertial range for $k < k_0$. The time unit in our simulations is set by the computational box size and sound speed, i.e., $t_1 = \sqrt{3}/k_1$.

As is well known, free decay of MHD turbulence implies an increase of the magnetic eddy size with decreasing magnetic energy density. Figure 2 illustrates this fact in our simulations. We display the y component of the magnetic field on the periphery of the domain during stages of its evolution after equipartition has been reached and driving
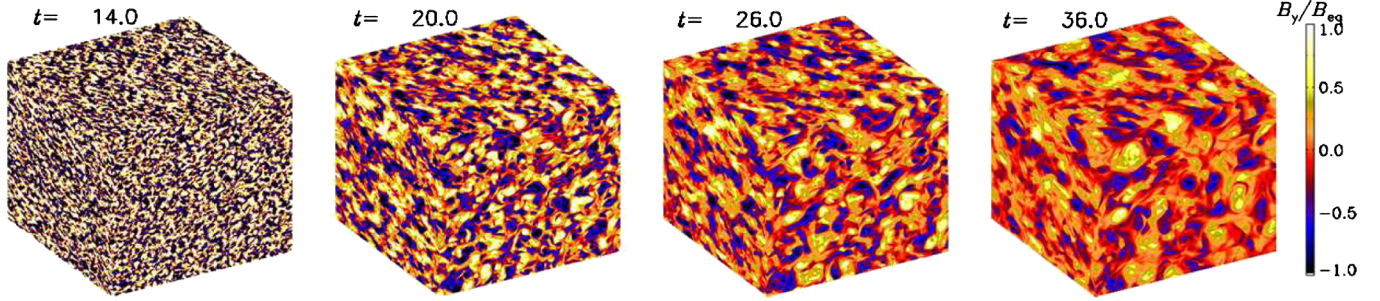
FIG. 2 (color online). Evolution of the turbulent magnetic field after turning off the forcing at time $t = 14t_1$. The B_y component is shown on the periphery of the computational domain.

was switched off, in the case when the magnetic energy was injected at some typical scale.

The characteristic time scales for the qualitative changes in the magnetic field distribution is approximately equal to $20t_1 \simeq 165\gamma\lambda_H$—a value that exceeds slightly the Hubble time-scale, λ_H/c, for the electroweak phase transition.

A. Development toward equipartition

We first examine how long it takes for forced MHD turbulence to establish equipartition between the magnetic and kinetic energy densities, i.e. where $v_A \simeq v_0$. Of course, the evolution of the magnetic energy spectrum is strongly scale dependent. We first address the case when the magnetic field is "created" at a typical scale k_0^{-1}, corresponding to the largest bubble. The Alfvén velocity of this field is close to the maximal value allowed by the BBN bound, i.e. $v_{A,\text{in}} \simeq 0.3$. In this case 10% of the available vacuum energy has been somehow transformed into magnetic energy before or during the phase transition. We perform our simulations with zero initial velocity perturbations. Such initial conditions may apply to the generation of turbulent motions during a phase transition via MHD processes, while the magnetic field was generated prior to that, for example, through quantum fluctuations [9,10]. In this case the evolution of magnetic and kinetic energy spectra during the first stages of MHD coupling are shown in Fig. 3. Taking into account that the largest bubble size must be a typical length scale for turbulence, our initial conditions imply that at $k = k_0$ equipartition is reached almost instantaneously. Larger scales need substantially longer times to establish equipartition. The initial evolution of magnetic energy spectra is shown in Fig. 4.

In our phenomenological description it has been assumed [45,51] that bubble collisions and nucleation lead to the development of turbulent motions, and the kinetic energy spectrum has been approximated as Kolmogorov-like in the inertial range ($E_K \propto k^{-5/3}$) and by a white noise spectrum ($E_K \propto k^2$) for $k < k_0$. As noted above, our simulations cannot adequately describe the inertial range and thus we cannot expect to see a Kolmogorov-like spectrum. On the other hand, the large-scale configuration of the velocity field is well approximated by white noise; see

Figs. 4–6. This agrees with what is predicted in the phenomenological approach.

We note that the kinetic energy spectrum grows faster right after the driving is switched on. In particular, after t_1, the r.m.s. velocity increases from zero to 0.17 while approaching 0.21 after $20t_1$. At $v_0 \sim 0.8v_A$ we assume that equipartition is reached and, by switching off the driving, we allow the turbulence to enter the second, free-decay stage.
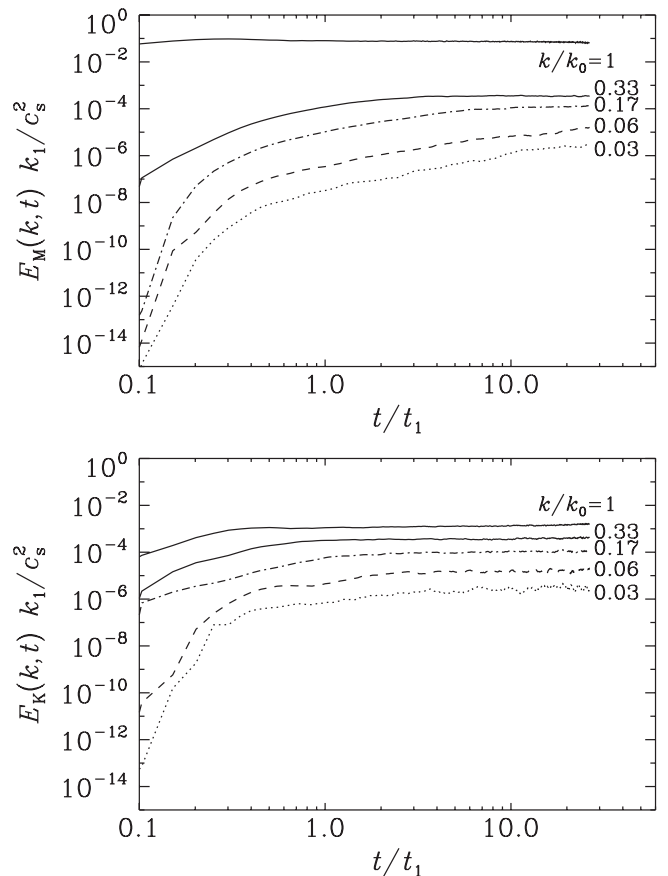

FIG. 3. Evolution of the magnetic energy spectral density $E_M(k, t)$ (upper panel) and kinetic energy spectral density $E_K(k, t)$ (lower panel) for different values of $k/k_0 = 0.03$, 0.06, 0.17, 0.33, and 1. The spectra are normalized such that $\int E_M(k, t)dk = \langle u^2 \rangle/2$.
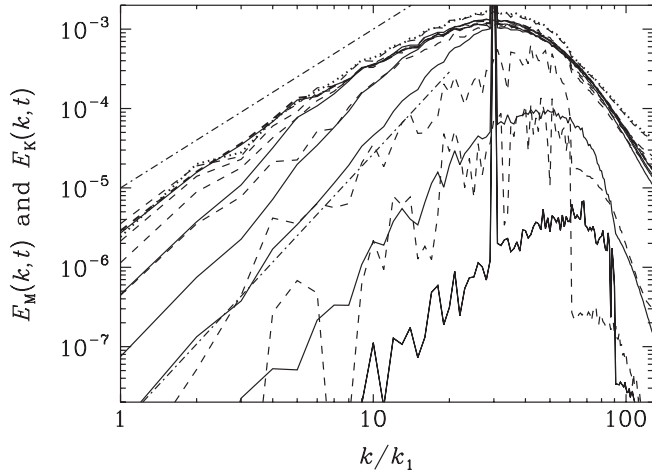
FIG. 4. The initial temporal evolution of magnetic energy spectra $E_M(k)$ [solid lines at $t/t_1 = 0.1$, 0.2, 0.5, 1.5, 5, and 25, with (smoothed) $E_M(k)$ at $k = 10k_1$ increasing as t increases] are shown before the field reaches equipartition with the kinetic energy density. For comparison, kinetic energy spectra are shown for the same times (dashed lines). Thick lines (solid and dashed) indicate the last time, $25t_1$. Straight dash-dotted lines have slopes 2 and 4. The box turnover time is $15t_1$ and is reached only for the last time shown.

B. Free decay of MHD turbulence

The free decay of turbulence is shown in Figs. 5 and 6 for two different initial configurations of the magnetic field. In both cases we perform MHD simulations after the driving force was switched off and free decay occurred.
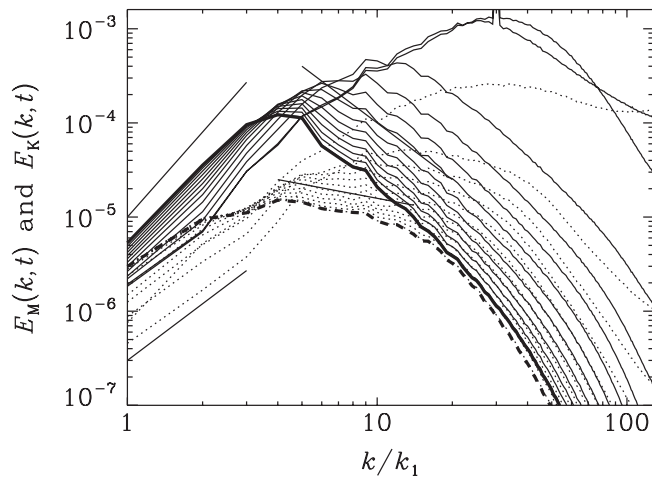
FIG. 5. Magnetic (solid line) and kinetic (dashed line) energy spectra in 12 regular time intervals of $4t_1$ after having turned off the forcing, with (smoothed) spectra at $k = 50k_1$ decreasing as t increases. $\nu = \eta = 10^{-4}$ in units of $(k_1^2 t_1)^{-1}$. The straight lines have slopes 3, 2, -2, and $-1/2$, with the first two near $k = k_1$ and the last two near $k = 10k_1$. Thickest lines (solid and dashed) indicate the last time, which is $44t_1$ since turning off the forcing. The intermediate thickness solid line, the highest or almost highest line for $k/k_1 > 10$, is the initial magnetic spectrum for this computation.
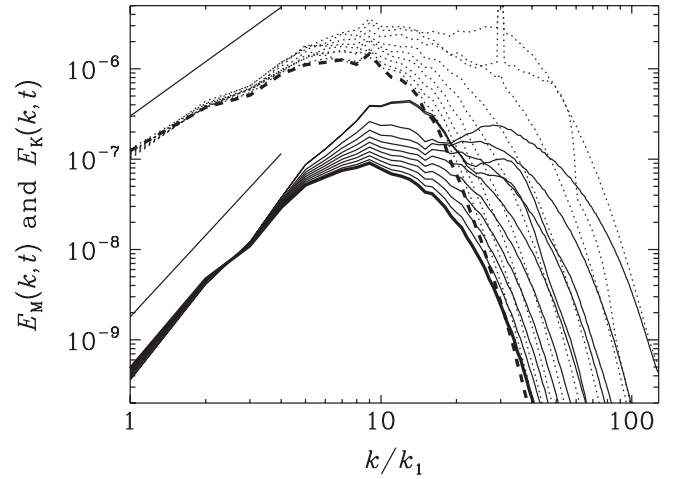

FIG. 6. Same as Fig. 5, but for a case where the initial magnetic field had a k^4 spectrum close to equipartition with the velocity field, and then the forcing was turned off. Results are shown for 9 times at intervals of $6t_1$. $\nu = \eta = 10^{-4}$ in units of $(k_1^2 t_1)^{-1}$. The straight lines have slopes 2 and 3. Thickest lines (solid and dashed) indicate the last time, which is $48t_1$ since turning off the forcing. The intermediate thickness solid line, the highest solid line for $5 < k/k_1 < 10$, is the initial magnetic spectrum for this computation.

The first case corresponds to the process described above, so it was preceded by magnetic field injection into the turbulent plasma at the scale of the largest bubbles or turbulent eddies. The field was then allowed to decay, leading to the development of near equipartition between the magnetic and turbulent energies. The second case corresponds to an initial configuration of a random magnetic field with a k^4 spectrum. In contrast to the first case, the process here can be roughly described as turbulent kinetic energy injection into the magnetized plasma. In this case we approximate the magnetic field spectrum at large scales by the steep Batchelor spectrum ($E_M \propto k^4$). Of course, the real situation during the phase transition is somewhere in between. If the magnetic field was generated during the phase transition through bubble collisions [15] the same process of bubble collisions leads to the generation of turbulent motions (vorticity perturbations). Thus, strictly speaking, we cannot split the turbulent motions and magnetic field generation and evolution. If the magnetic field was created before the phase transition, it affects the bubble collisions (locally inserting a preferred direction). As a result, the process of generation of turbulent motions is affected and this backreacts onto the magnetic field configuration itself.

The first case—injection of magnetic energy into the turbulent plasma—provides a suitable setting for magnetic field generation through the mechanism described in Ref. [52], where the correlation length of the magnetic field is naturally set by the size of the phase transition bubbles. The second case with an established magnetic

field spectrum is more appropriate for the causal mechanisms discussed in Ref. [34].

Figures 5 and 6 show a distinctive difference between the turbulent states developed after the injection of the magnetic energy through a single-mode magnetic field, and the injection of kinetic energy in the existing magnetic field with smooth magnetic spectral energy-density distribution. A major difference is revealed in the spectral distribution of magnetic and velocity fields at large scales. At large scales, the spectral slopes are approximately 2 for kinetic energy and around 3 for magnetic energy. Therewith, the spectral distribution of kinetic energy shows less sensitivity to initial conditions and develops a shape close to white noise with $E_k \propto k^2$. The final configuration of the large-scale magnetic field slightly differs as a consequence of the initial conditions. In the case of magnetic energy injection (Fig. 5) the spectral slope is shallower than 3, and tends to establish a white noise spectrum, while the case of kinetic energy injection (Fig. 6) most probably results in the steep Batchelor spectrum.

In all cases, throughout the free-decay stage, the peak of the magnetic field spectral energy density drifts to smaller wave numbers as $k_{\text{peak}}(t) \propto t^{-1/2}$. At the same time magnetic power decreases as $E_M(k, t) \propto t^{-1}$. Accounting for these scalings and noting that we use conformal time, the temporal scaling in the case of an expanding Universe is somewhat slower than that in the case of laboratory grid turbulence where $E_K \propto t_{\text{phys}}^{-n}$ with exponents between $n = 1.13$ [53] and 1.25 [54].

Simulations show that equipartition between kinetic and magnetic energies is sustained throughout the free decay stage of the turbulence. Therewith, at any given point in time, the kinetic energy spectrum peaks at the same wave number as the magnetic energy spectrum. However, it seems that properties of the turbulent states developed through free decay depend on the method of their generation. The power spectrum of the turbulence developed after injection of a single-mode magnetic field energy peaks at $k_{\text{max}} \sim 3k_1$, while injection of kinetic energy into an existing magnetic configuration leads to a turbulent state with power spectrum peaking at $k_{\text{max}} \sim 9k_1$. Hence, it seems that, in general, the characteristic length scale of the turbulence is sensitive to the initial driver: kinetic drivers result in smaller-scale turbulence states as compared to the case of magnetic field drivers.

IV. CONCLUSIONS

In this paper we have presented results from direct numerical simulations of primordial magnetic field evolution during cosmological phase transitions. These simulations account for the expansion of the Universe. Simulations were performed to model two different stages of primordial magnetic field evolution, the first stage when phase transition processes drive turbulence, and the second stage when free decay occurs.

We show that different types of initial conditions (drivers) lead to rapid development of a turbulent state close to equipartition. During the following stage we model the free decay of these turbulence configurations. We study the development during this free decay stage and analyze characteristic parameters of the slowly varying power spectrum of the turbulence. We assume that the properties of the turbulence configurations modeled in our numerical experiments are similar to those of cosmological primordial turbulence.

Our simulations allow us to estimate the spectral indices of the large-scale distribution of the kinetic and magnetic field energies in developed turbulence. It seems that the final configuration of primordial magnetic field depends on the initial conditions that must be determined by the phase transition physics. On the other hand, the kinetic energy density of the developed state does not retain any information about the initial conditions and hence is not sensitive to the details of the phase transition. The spectral index of the kinetic energy at large scales can be well approximated as 2 (white noise spectrum), while the magnetic energy-density spectral index ranges between 2 and 4 depending on the initial conditions. Similar spectral indices for the large-scale magnetic field are well established for laboratory turbulence, see Ref. [55]. Note that simulations in a finite periodic domain may suffer from the fact that originally disconnected and causally independent regions come into causal contact within one box turnover time, which, based on the scale of the domain, is $(v_0 k_1)^{-1}$. For the case shown in Fig. 4, this time is about $15t_1$, but the effective time can be even shorter owing to the effects of acoustic and Alfvén waves.

Our numerical results allow us to estimate typical timescales for decaying free turbulence. It seems that cosmological turbulence decays slightly slower then classical grid turbulence in laboratory experiments. Although we took a rather small damping wave number, we cannot expect the establishment of a Kolmogorov-like spectrum at small scales. We see a fast decorrelation of turbulence at small scales. We note that the phenomenological approaches developed in Refs. [23,28] imply a fast Kraichnan-like decorrelation of turbulence. Consequently, only the large-scale or peak-scale magnetic field results may have cosmological significance and contribute observable signatures, such as gravitational wave generation and/or CMB anisotropy production.

We have considered the case of nonhelical turbulence. The presence of weak initial helicity can significantly change the development of turbulence. This is because magnetic helicity is a conserved quantity in the limit of large magnetic Reynolds numbers and can inverse cascade to larger scales [56,57], which could be cosmologically significant. This process has been confirmed through numerous simulations [25,26,31,47].

Summarizing, we find that the generation of a magnetic field at phase transition scales will lead to the development

of turbulent motions, and, in the case of the electroweak phase transition, this turbulence has an observable signature in the form of a gravitational wave signal.

ACKNOWLEDGMENTS

[1] L. M. Widrow, Rev. Mod. Phys. **74**, 775 (2002).

[2] J. P. Vallée, New Astron. Rev. **48**, 763 (2004).

[3] M. Giovannini, Lect. Notes Phys. **737**, 863 (2008).

[4] R. Beck, in *Proceedings of the 4th International Meeting on High Energy Gamma-Ray Astronomy*, edited by F. A. Aharonian, W. Hofmann, and F. Rieger AIP Conf. Proc. No. 1085 (AIP, New York, 2009), p. 83.

[5] A. Neronov and D. Semikoz, Phys. Rev. D **80**, 123012 (2009).

[6] K. Subramanian, Astron. Nachr. **331**, 110 (2010).

[7] W. Fischler, B. Ratra, and L. Susskind, Nucl. Phys. **B259**, 730 (1985).

[8] M. S. Turner and L. M. Widrow, Phys. Rev. D **37**, 2743 (1988).

[9] B. Ratra, Astrophys. J. **391**, L1 (1992).

[10] K. Bamba and J. Yokoyama, Phys. Rev. D **69**, 043507 (2004); J. Martin and J. Yokoyama, J. Cosmol. Astropart. Phys. 01 (2008) 025; G. Lambiase, S. Mohanty, and G. Scarpetta, J. Cosmol. Astropart. Phys. 07 (2008) 019; K. Bamba, N. Ohta, and S. Tsujikawa, Phys. Rev. D **78**, 043524 (2008), and references therein.

[11] B. Ratra, Caltech Report No. GRP-287/CALT-68-1751, 1991, available at www.phys.ksu.edu/personal/ratra/.

[12] V. Demozzi, V. Mukhanov, and H. Rubinstein, J. Cosmol. Astropart. Phys. 08 (2009) 025.

[13] S. Kanno, J. Soda, and M.-a. Watanabe, J. Cosmol. Astropart. Phys. 12 (2009) 009; R. Enami, H. Firouzjahi, and M. S. Movahed, Phys. Rev. D **81**, 083526 (2010).

[14] S. Maeda, S. Mukohyama, and T. Shiromizu, Phys. Rev. D **80**, 123538 (2009).

[15] E. R. Harrison, Mon. Not. R. Astron. Soc. **147**, 279 (1970); T. Vachaspati, Phys. Lett. B **265**, 258 (1991); A. Brandenburg, K. Enqvist, and P. Olesen, Phys. Rev. D **54**, 1291 (1996); J. M. Cornwall, Phys. Rev. D **56**, 6146 (1997); G. Sigl, A. V. Olinto, and K. Jedamzik, Phys. Rev. D **55**, 4582 (1997); A.-C. Davis and K. Dimopoulos, Phys. Rev. D **55**, 7398 (1997); M. Joyce and M. E. Shaposhnikov, Phys. Rev. Lett. **79**, 1193 (1997); M. Hindmarsh and A. Everett, Phys. Rev. D **58**, 103505 (1998); D. Grasso, Nucl. Phys. B, Proc. Suppl. **110**, 189 (2002); D. Boyanovsky, M. Simionato, and H. J. de Vega, Phys. Rev. D **67**, 023502 (2003); L. Campanelli and M. Giannotti, Phys. Rev. D **72**, 123001 (2005); L. Hollenstein, C. Caprini, R. Crittenden, and R. Maartens, Phys. Rev. D **77**, 063517 (2008); A. Díaz-Gil, J. García-Bellido, M. García Pérez, and A. González-Arroyo, J. High Energy Phys. 07 (2008) 043, and references therein.

[16] M. Giovannini, Classical Quantum Gravity **23**, R1 (2006).

[17] T. Kahniashvili and B. Ratra, Phys. Rev. D **75**, 023002 (2007); D. G. Yamazaki, K. Ichiki, T. Kajino, and G. J. Mathews, Phys. Rev. D **77**, 043005 (2008); D. G. Yamazaki, K. Ichiki, K. Toshitaka, and G. J. Mathews, Mod. Phys. Lett. A **23**, 1695 (2008); F. Finelli, F. Paci, and D. Paoletti, Phys. Rev. D **78**, 023510 (2008); J. R. Kristiansen and P. G. Ferreira, Phys. Rev. D **77**, 123004 (2008); D. Paoletti, F. Finelli, and F. Paci, Mon. Not. R. Astron. Soc. **396**, 523 (2009), and references therein.

[18] S. Sethi, Mon. Not. R. Astron. Soc. **342**, 962 (2003); L. Campanelli, A. D. Dolgov, M. Giannotti, and F. L. Villante, Astrophys. J. **616**, 1 (2004); A. Kosowsky, T. Kahniashvili, G. Lavrelashvili, and B. Ratra, Phys. Rev. D **71**, 043006 (2005); M. Giovannini and K. E. Kunze, Phys. Rev. D **78**, 023010 (2008); T. Kahniashvili, Y. Maravin, and A. Kosowsky, Phys. Rev. D **80**, 023009 (2009), and references therein.

[19] M. Demianski and A. G. Doroshkevich, Phys. Rev. D **75**, 123517 (2007); A. Bernui and W. S. Hipolito-Ricaldi, Mon. Not. R. Astron. Soc. **389**, 1453 (2008); T. Kahniashvili, G. Lavrelashvili, and B. Ratra, Phys. Rev. D **78**, 063012 (2008); P. K. Samal, R. Saha, P. Jain, and J. P. Ralston, Mon. Not. R. Astron. Soc. **396**, 511 (2009); J. Kim and P. Naselsky, J. Cosmol. Astropart. Phys. 07 (2009) 041; L. R. Abramo, A. Bernui, and T. S. Pereira, J. Cosmol. Astropart. Phys. 12 (2009) 013, and references therein.

[20] T. R. Seshadri and K. Subramanian, Phys. Rev. Lett. **103**, 081303 (2009); C. Caprini, F. Finelli, D. Paoletti, and A. Riotto, J. Cosmol. Astropart. Phys. 06 (2009) 021.

[21] D. Grasso and H. R. Rubinstein, Phys. Rep. **348**, 163 (2001).

[22] D. V. Deriagin, D. Grigor'ev, V. Rubakov, and M. Sazhin, Mon. Not. R. Astron. Soc. **229**, 357 (1987).

[23] T. Kahniashvili, A. G. Tevzadze, and B. Ratra, arXiv:0907.0197.

[24] S. Wang, Phys. Rev. D **81**, 023002 (2010), and references therein.

[25] R. Banerjee and K. Jedamzik, Phys. Rev. D **70**, 123003 (2004).

[26] M. Christensson, M. Hindmarsh, and A. Brandenburg, Phys. Rev. E **64**, 056405 (2001).

[27] N. E. Haugen, A. Brandenburg, and W. Dobler, Phys. Rev. E **70**, 016308 (2004).

[28] C. Caprini, R. Durrer, and E. Fenu, J. Cosmol. Astropart. Phys. 11 (2009) 001; C. Caprini, R. Durrer, and G. Servant, J. Cosmol. Astropart. Phys. 12 (2009) 024.

[29] D. Biskamp, *Magnetohydrodynamic Turbulence* (Cambridge University, Cambridge, England, 2003).

[30] M. K. Verma, Phys. Rep. **401**, 229 (2004).

[31] M. Christensson, M. Hindmarsh, and A. Brandenburg, Astron. Nachr. **326**, 393 (2005).

[32] A. Kosowsky and M. S. Turner, Phys. Rev. D **47**, 4372 (1993).

[33] C. J. Hogan, Phys. Rev. Lett. **51**, 1488 (1983).

[34] R. Durrer and C. Caprini, J. Cosmol. Astropart. Phys. 11 (2003) 010.

[35] G. K. Batchelor, Proc. R. Soc. A **201**, 405 (1950).

[36] G. K. Batchelor and I. Proudman, Proc. R. Soc. A **248**, 369 (1956).

[37] A. P. Kazantsev, Sov. Phys. JETP **26**, 1031 (1968).

[38] A. A. Schekochihin, S. C. Cowley, J. L. Maron, and J. C. McWilliams, Phys. Rev. Lett. **92**, 064501 (2004).

[39] http://pencil-code.googlecode.com/

[40] K. Kajantie, M. Laine, K. Rummukainen, and M. Shaposhnikov, Phys. Rev. Lett. **77**, 2887 (1996).

[41] J. Rosiek, Phys. Rev. D **41**, 3464 (1990), and references therein.

[42] M. Laine, Nucl. Phys. **B481**, 43 (1996); **B548**, 637 (1999); J. M. Cline and K. Kainulainen, Nucl. Phys. **B482**, 73 (1996); J. M. Cline and G. D. Moore, Phys. Rev. Lett. **81**, 3315 (1998); M. Losada, Nucl. Phys. **B537**, 3 (1999), and references therein.

[43] G. De Risi, T. Harko, F. S. N. Lobo, and C. S. J. Pun, Nucl. Phys. **B805**, 190 (2008); E. S. Fraga and A. J. Mizher, Nucl. Phys. **A820**, 103c (2009); A. Bessa, E. S. Fraga, and B. W. Mintz, Phys. Rev. D **79**, 034012 (2009); K.-F. Liu, *SSP09 Symposium, Taipei, Taiwan, June 2009* (to be published); C. Bonati *et al.*, Nucl. Phys. **A820**, 243c (2009); D. J. Schwarz and M. Stuke, J. Cosmol. Astropart. Phys. 11 (2009) 025, and references therein.

[44] R. Apreda *et al.*, Classical Quantum Gravity **18**, L155 (2001); J. F. Dufaux *et al.*, Phys. Rev. D **76**, 123517 (2007); S. J. Huber and T. Konstandin, J. Cosmol. Astropart. Phys. 05 (2008) 017; 09 (2008) 022.

[45] A. Nicolis, Classical Quantum Gravity **21**, L27 (2004).

[46] A. S. Monin and A. M. Yaglom, *Statistical Fluid Mechanics* (MIT, Cambridge, MA, 1975).

[47] A. Brandenburg, K. Enqvist, and P. Olesen, Phys. Rev. D **54**, 1291 (1996).

[48] A. Brandenburg and W. Dobler, Comput. Phys. Commun. **147**, 471 (2002).

[49] A. Brandenburg, in: *Advances in Nonlinear Dynamos*, edited by A. Ferriz-Mas and M. Nunez (Taylor and Francis, London, 2003), pp. 269–344.

[50] W. Dobler, M. Stix, and A. Brandenburg, Astrophys. J. **638**, 336 (2006).

[51] M. Kamionkowski, A. Kosowsky, and M. S. Turner, Phys. Rev. D **49**, 2837 (1994).

[52] T. Stevens and M. B. Johnson, Phys. Rev. D **80**, 083011 (2009); E. M. Henley, M. B. Johnson, and L. S. Kisslinger, Phys. Rev. D **81**, 085035 (2010).

[53] P. A. Krogstad, and P. A. Davidson, J. Fluid Mech. **642**, 373 (2010).

[54] H. S. Kang, S. Chester, and C. Meneveau, J. Fluid Mech. **480**, 129 (2003); N. E. L. Haugen and A. Brandenburg, Phys. Rev. E **70**, 026405 (2004).

[55] P. A. Davidson, *Turbulence* (Oxford University Press, New York, 2004).

[56] U. Frisch, A. Pouquet, J. Léorat, and A. Mazure, J. Fluid Mech. **68**, 769 (1975).

[57] D. Biskamp, *Nonlinear Magnetohydrodynamics* (Cambridge University, Cambridge, England, 1993).